Astron. Nachr./AN **xxx** (xxxx) x, xxx–xxx

Future magnetic fields studies using the Planck surveyor experiment

TORSTEN A. ENSSLIN[1], ANDRÉ WAELKENS[1], CORINA VOGT[1,2], and ALEXANDER A. SCHEKOCHIHIN[3]

[1] Max-Planck-Institute für Astrophysik, Karl-Schwarzschild-Str. 1, 85741 Garching, Germany
[2] Stichting ASTRON, P.O. Box 2, NL–7990 AA Dwingeloo, The Netherlands
[3] DAMTP/CMS, University of Cambridge, Wilberforce Road, Cambridge CB3 0WA, United Kingdom

Received; accepted; published online

Abstract. The Planck mission will permit measurements of the polarization of the cosmic microwave background and of polarized foregrounds such as our own Galaxy with an unprecedented combination of accuracy and completeness. This will provide information on cosmological and galactic magnetic fields. The latter can be studied in detail via nearly Faraday-rotation free synchrotron and polarized dust emission. Methods are discussed to extract physically relevant information on the magnetic turbulence from Planck data and other measurements.

Key words: space vehicles: instruments – cosmic microwave background – polarization – ISM: magnetic fields – Galaxy: structure

1. The Planck surveyor mission

1.1. The experiment

"Planck is a mission of the European Space Agency designed to answer key cosmological questions. Its ultimate goal is to determine the geometry and content of the Universe, and which theories describing the birth and evolution of the Universe are correct. To achieve this ambitious objective, it will observe the Cosmic Microwave Background radiation (CMB), emitted about 13 thousand million years ago, just 400,000 years after the Big Bang. Today the CMB permeates the Universe and is observed to have an average temperature of 2.726 K. Small deviations from this average value (the so-called anisotropies), observable at angular scales larger than a few arcminutes, encode a wealth of information on the properties of the Universe in its infancy. The objective of Planck is to measure these properties with an unprecedented accuracy and level of detail." (*The Planck Bluebook* (2005)).

The Planck satellite will operate at the $2^{\rm nd}$ Lagrange point of the Sun-Earth system, with both Sun and Earth in the direction of the axis of the satellite, around which it rotates with 1 rotation per minute. Two sets of detectors will be on board, the HEMT receivers for the Low Frequency Instrument (LFI) ranging from 30 to 70 GHz and bolometers for the High Frequency Instrument (HFI) ranging from 100 to 860 GHz. Both instruments will have receivers sensitive to linear polarization.

The instrument beams will have resolutions of 5 to 30 $\rm arcmin$ and observe the sky with an inclination of $85°$ with respect to the spin axis. About every 60 rotations, the spin axis will be rearranged to a new direction within a $10°$ cone pointing towards the Sun. Within seven months, the complicated scanning strategy of Planck will have covered the full sky at least once everywhere, and two complete coverages are planned.

1.2. The data

The CMB is not the only microwave emitter measured by the instruments. Galactic synchrotron, free-free, and dust emission and extra-galactic sources contaminate the signal. Fortunately, nearly all of them have emission spectra which are very different from the CMB. The nine Planck spectral channels cover one and a half orders of magnitude in frequency. This is necessary to separate the different physical components observed by a combination of spectral decomposition and spatial filtering. Detailed properties of the detectors can be found in Table 1. The resulting physical component maps can then be analyzed separately according to their nature. Here, only the CMB and the Galactic emission components are of relevance.

Correspondence to: ensslin@mpa-garching.mpg.de

Table 1. Reproduced from *The Planck Bluebook* (2005).

SUMMARY OF PLANCK INSTRUMENT CHARACTERISTICS

INSTRUMENT CHARACTERISTICS	LFI			HFI					
Detector Technology	HEMT arrays			Bolometer arrays					
Center Frequency [GHz]	30	44	70	100	143	217	353	545	857
Bandwidth ($\delta\nu/\nu$)	0.2	0.2	0.2	0.33	0.33	0.33	0.33	0.33	0.33
Angular Resolution (arcmin)	33	24	14	10	7.1	5.0	5.0	5.0	5.0
δT/T per pixel (Stokes I)[a]	2.0	2.7	4.7	2.5	2.2	4.8	14.7	147	6700
δT/T per pixel (Stokes Q &U)[a]	2.8	3.9	6.7	4.0	4.2	9.8	29.8	...	...

[a] Goal (in μK/K) for 14 months integration, 1 σ, for square pixels whose sides are given in the row Angular Resolution.

2. Primordial magnetic fields

Particle physics scenarios exist which predict weak primordial magnetic fields, but usually on very small scales (see papers in these proceedings by M. Gasperini, by D. Dario, by K. Takahashi, and by D. Sokoloff). K. Subramanian and also T. Kahniashvili (these proceedings) take the pragmatic approach to assume that some primordial fields exist and to investigate its observable signatures. The same approach will be used in the following.

2.1. Imprint in power spectra

A uniform primordial magnetic field would break the cosmic isotropy. Since this can be tested via CMB data, nG limits on a uniform field were derived from WMAP and other data, which certainly can be tightened by Planck (see Giovannini (2005) for a discussion).

A tangled primordial magnetic field would lead to the presence of Alfvén waves in the primordial plasma — provided the field is dynamically significant and there is a non-empty scale interval between the scale of the field and the ion Larmor radius. The Alfvénic oscillations should imprint characteristic signatures onto the CMB. On large scales, the development of these oscillations is suppressed due to the very limited distance the relatively slow Alfvén waves can have traveled for sub-equipartition fields ($B \ll 3\,\mu$G from constraints of Big Bang nucleosynthesis). On small scales, "oscillations of ... Alfvén waves get overdamped in the radiation diffusion regime, resulting in frozen-in magnetic field perturbations" (Jedamzik et al. (1998)). This freezing allows the magnetic fluctuations to survive until recombination and then to produce temperature fluctuations.

Subramanian & Barrow (1998) estimate that fields with power-law spectra close to scale-invariance of 3 nG result in $10\,\mu$K temperature fluctuations on multipole scales of $l \sim 1000 - 3000$ (below 10 arcmin). On sufficiently small scales, the magnetically induced power spectrum will easily be above the CMB spectrum of the acoustic oscillations due to Silk damping of the latter. Subramanian & Barrow (1998) find that for the above parameters this happens at $l \gtrsim 2000$.

However, the identification of primordial fields using temperature fluctuations observed by Planck will be challenging. Planck will have an angular resolution down to 5 arcmin ($l \sim 2000$). Therefore, magnetic fields have to be stronger than assumed above in order for them to exceed the acoustic fluctuations at these scales and be detectable. And even if Planck detects excess power at those scales, a large number of competing explanations is expected.

A unique identification of CMB fluctuations due to magnetic fields may be possible via the induced polarization signature and/or non-Gaussian statistics. However, since these are more subtle measurements, their detection in Planck data is probably also very challenging. We (the authors) do not have a clear picture of the feasibility of uniquely identifying magnetic contributions to the CMB fluctuations.

Nevertheless, Planck will be able to constrain primordial magnetic field scenarios since its measurements can always be used to set upper limits on magnetically induced fluctuations.

2.2. Faraday rotation

A nice signature of primordial magnetic fields would be an induced Faraday rotation of the CMB polarization. This effect rotates polarization vectors with a characteristic λ^2 dependence, which means that the lowest frequency channel of Planck will be best suited for such a signal (30 GHz). The technical specification of Planck requires an accuracy of polarization angle measurements of about 1 degree. This translates into a sensitivity in rotation measure of RM$\sim 100\,\mathrm{rad/m^2}$.

The Faraday-rotation signal from nG magnetic fields is expected to be about one degree rotation at 30 GHz (see e.g., Kosowsky et al. (2005)). However, since the CMB polarization is a weak, small-scale signal, the changes due to Faraday rotation are even weaker and are also on small scales. The expected signal peaks with $0.1\,\mu$K polarization fluctuations at $l \sim 10^4$. These will be unobservable for Planck due to beam smearing effects (the 30 GHz system of Planck will be limited to 33 arcmin resolution $l \sim 400$), and due to the the overwhelmingly bright and highly polarized Galactic synchrotron emission at those frequencies extending to high latitudes. Usage of higher frequencies can decrease the Galactic synchrotron contamination at the price of an even stronger reduction of the wavelength-dependent Faraday-rotation signal.

In summary, a discovery of primordial magnetic fields via their Faraday effect is not to be expected from Planck.

3. Galactic magnetic fields

The study of primordial magnetic fields with Planck will be difficult, partly because of the Galactic synchrotron contamination. However, the strength of the Galactic foreground signal may open the possibility to study Galactic magnetic fields in great detail.

3.1. Synchrotron, Faraday, and dust polarimetry

Planck will be sensitive to magnetic fields $\boldsymbol{B}$ via

1. synchrotron emission ($\boldsymbol{B}_\perp$),
2. Faraday rotation ($B_{||}$),
3. and polarized dust emission ($\boldsymbol{B}_\perp/B_\perp$),

where $\perp$ and $||$ refer to the field component with respect to the line of sight.

Synchrotron emission is ideal for the study of galactic magnetic fields because the spatial distribution of relativistic electrons illuminating the fields should be smooth, due to their diffusivity, and can be measured by other means, e.g., via the inverse Compton scattering of CMB and starlight.

Faraday rotation is also ideal because the required spatial distribution of thermal electrons can be measured by other means (e.g., their free-free emission). Despite the expected high precision in determining polarization angles ($\sim 1^\circ$), Planck will only be sensitive to RM $> 100\,\mathrm{rad/m^2}$ due to its relatively high-frequency channels ($\geq$ 30 GHz). Nevertheless, Planck can provide "zero-wavelength" data for a multi-instrument Faraday campaign.

Polarized dust emission due to scattered or partially absorbed starlight (e.g., Fosalba et al. (2001)) or spinning elongated dust grains (e.g., Draine & Lazarian (1998)) might help to build and constrain models of the galactic field topology. However, it will be difficult to use this for quantitative investigations of Galactic magnetic fields, due to the complex dependence of the signal on the poorly known dust properties and spatial distribution.

3.2. Reconstruction of large-scale fields

Given the large amount of information that Planck and other polarimetry instruments will provide on tracers of Galactic magnetic fields, one might ask if a full reconstruction of the large-scale field based purely on observational data is possible. The polarimetry of synchrotron emission provides three observables: the Stokes parameters $I(\lambda)$, $Q(\lambda)$, and $U(\lambda)$, as functions of wavelength λ. The goal would be to reconstruct from these the three magnetic-field components $B_x(z)$, $B_y(z)$, and $B_z(z)$, which are functions of the coordinate along the line-of-sight z:

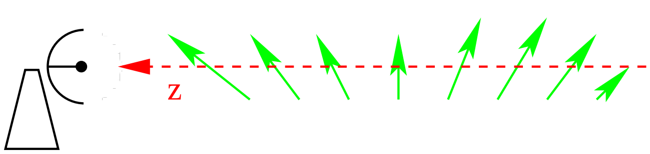

Do we have enough information to reconstruct $\boldsymbol{B}(z)$?

The observed Stokes parameters are given in terms of their emissivities

$$I(\lambda) = \int dz\, \varepsilon_I(z,\lambda),$$
$$P(\lambda) = \int dz\, \varepsilon_P(z,\lambda)\, \exp(2i\lambda^2\,\phi(z)),$$

where $P = Q + iU$ denotes the complex polarization, on which the rotation measure $\phi(z) \propto \int dz\, B_z(z)\, n_e(z)$ acts like a mathematical rotation operator. The emissivities are roughly given by combinations of the perpendicular magnetic field components:

$$\varepsilon_I \propto (B_x^2 + B_y^2)\, n_{\mathrm{CRe}},$$
$$\varepsilon_P \propto (B_x^2 - B_y^2 + 2iB_x B_y)\, n_{\mathrm{CRe}}.$$

The projection of the total intensity emission in the observation removes any spatial information. For the polarized emission, the frequency-dependent Faraday effect permits that spatial information imprints itself into the data. However, introducing the emissivity per Faraday depth

$$\varepsilon_P(\phi) = \int dz\, \varepsilon_P(z)\, \delta(\phi(z) - \phi)$$

permits the observable polarization to be expressed without any reference to the spatial distribution:

$$P(\lambda) = \int_{-\infty}^{\infty} d\phi\, \varepsilon_P(\phi,\lambda)\, \exp(2i\lambda^2\,\phi).$$

Therefore, a spatial reconstruction is impossible since spatial information is lost in the projection!

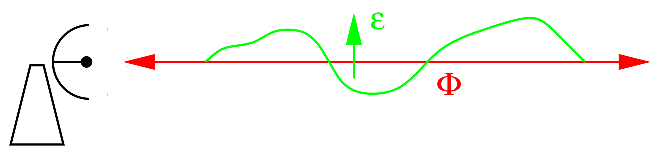

Do we have enough information to reconstruct $\varepsilon_P(\phi)$?

$P(\lambda)$, expressed as a function of the variable $a = 2\,\lambda^2$, and $\varepsilon_P(\phi)$ are Fourier transforms of each other. Knowing one function allows the reconstruction of the other. Unfortunately, measurements at negative values of $a = 2\,\lambda^2$ would be required to reconstruct the complex function $\varepsilon_P(\phi)$, but this is impossible. Thus, at best half of the information necessary for a reconstruction of $\varepsilon_P(\phi)$ is available.

Although the above equations cannot be inverted, the forward approach is possible: the construction of polarized emission maps from Galactic models.

The Fourier based formalism of Faraday rotation allows a computationally efficient calculation of spectral cubes of polarized maps using the fast Fourier transform. Waelkens (2005) implemented the generation of maps of Stokes parameters I, Q, and U using a nested spherical pixelization (HEALPix, Górski et al. (2005)) in order to treat beam-depolarization effects accurately. This code requires as inputs

– a Galactic electron model (Cordes & Lazio (2002)),
– a Galactic cosmic-ray electron model,
– a Galactic magnetic-field model.

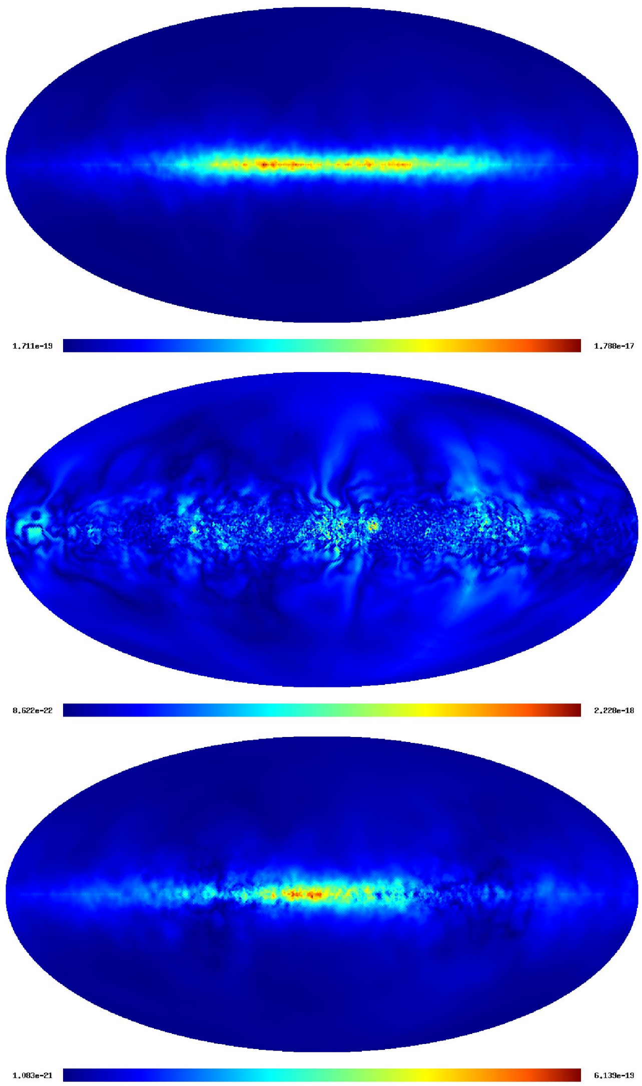

Fig. 1. Simulated Galactic total (top) and polarized (middle) intensity at 1.4 GHz and polarized intensity at the lowest Planck frequency of 30 GHz (bottom) calculated with the code of Waelkens (2005). Note the Faraday depolarization effects in the low frequency map that disappear at high frequencies. The units are $\mathrm{erg}/(\mathrm{s\,cm^2\,Hz\,str})$.

Fig. 1 shows synthetic emission maps produced by the code for a very simplistic magnetic field configuration (a logarithmic spiral without field reversals but with an added random component). Surprisingly, the simulated maps already reproduce many features of the observed ones, despite the simplicity of the model used. For instance, the observed Faraday-depolarization channels, which contribute to the low fractional polarization in the Galactic plane, seem also to be present in the simulation.

4. Studying magnetic turbulence

The Planck-polarization maps may allow a study of properties of MHD turbulence in the Galaxy with a spatial resolution not achievable in numerical simulations and a richness in detail not reachable in analytical investigations.

But how to extract physically meaningful signals? In order to better understand the technical details of signal extraction, we explain first, how magnetic power spectra could be extracted from Faraday rotation maps. Then we show that higher-order statistical properties of the magnetic turbulence may be measurable from Planck synchrotron-polarization data.

4.1. Faraday rotation & magnetic power spectra

Extended and polarized radio sources in galaxy clusters can be used to study magnetic turbulence in the intergalactic medium. The Faraday rotation map of Hydra A was analyzed by Vogt & Enßlin (2005) to determine the magnetic power spectrum within the Faraday screen in front of it (see Fig. 2). This analysis was based on

- homogeneous, isotropic, and divergence-free magnetic turbulence,
- known cluster geometry (window function), and
- Bayes' theorem connecting probabilistically the model spectra and the observed RM fluctuations.

The incorporation of these assumptions in the analysis is explained in the following.

Homogeneous magnetic turbulence is best studied using the magnetic-field correlation tensor

$$M_{ij}(\boldsymbol{r}) = \langle B_i(\boldsymbol{x})\, B_j(\boldsymbol{x}+\boldsymbol{r})\rangle,$$

whose Fourier space representation is

$$\hat{M}_{ij}(\boldsymbol{k}) = \frac{1}{V}\langle \hat{B}_i(\boldsymbol{k})\, \overline{\hat{B}_j(\boldsymbol{k})}\rangle\,.$$

In general, this tensor would be described by nine functions defined in the three-dimensional k-space. However, assuming isotropy and $\boldsymbol{\nabla}\cdot\boldsymbol{B} = 0$, it reduces to

$$\hat{M}_{ij}(\boldsymbol{k}) = \frac{1}{2}\,\hat{w}(k)\,\left(\delta_{ij} - \frac{k_i\,k_j}{k^2}\right) - i\varepsilon_{ijm}\,\frac{k_m}{k}\,\hat{H}(k)\,,$$

which depends only on two functions of $k = |\boldsymbol{k}|$:

3-d power spectrum: $\hat{w}(k) = \frac{1}{V}\langle \hat{\boldsymbol{B}}(\boldsymbol{k})\cdot\overline{\hat{\boldsymbol{B}}(\boldsymbol{k})}\rangle$

3-d magnetic helicity: $\hat{H}(k) = \frac{i}{2\,V\,k}\langle \hat{\boldsymbol{B}}(\boldsymbol{k})\cdot(\overline{\hat{\boldsymbol{B}}(\boldsymbol{k})}\times\boldsymbol{k})\rangle$.

Faraday rotation measures the line-of-sight projected magnetic field

$$\mathrm{RM}(\boldsymbol{x}_\perp) = a_0 \int_{z_s(\boldsymbol{x}_\perp)}^{\infty} dz\; n_e(\boldsymbol{x})\, B_z(\boldsymbol{x})\,,$$

where $a_0 = e^3/2\pi m_e^2 c^4$. The RM autocorrelation function

$$C_{\mathrm{RM}}(\boldsymbol{r}_\perp) = \langle \mathrm{RM}(\boldsymbol{x}_\perp)\, \mathrm{RM}(\boldsymbol{x}_\perp + \boldsymbol{r}_\perp)\rangle$$

is, therefore, connected to the magnetic-field correlation tensor. Although we would need two measurable correlation functions in order to reconstruct the full tensor, the symmetric part of the tensor is fully encoded in the data (Enßlin & Vogt 2003):

$$\hat{C}^{\mathrm{obs}}_{\mathrm{RM}}(\boldsymbol{k}_\perp) = \frac{1}{2}\, a_0^2\, n_{\mathrm{e},0}^2\, L\, \hat{w}(|\boldsymbol{k}_\perp|)\,.$$

Here $n_{\mathrm{e},0}$ is a characteristic electron density within the Faraday screen of depth L. Since the information contained in the power spectrum alone (and not the helicity) determines the signal, the spectrum can be inferred from a single observable.

For real data, the situation is a bit more complicated, since the limited size of the tested volume imprints on the measured correlation function. This can be described by a window function $W(\boldsymbol{x})$, which contains the geometrical information on the variation of the cluster electron density and the limited lateral size of the radio source image. The connection between magnetic-field and RM spectra becomes:

$$\hat{C}^{\rm obs}_{\rm RM}(\boldsymbol{k}_\perp) = \frac{1}{2}\, a_0^2\, n_{\rm e,0}^2\, L \int d^3q\ \hat{w}(q)\ \frac{q_\perp^2}{q^2}\, W(\boldsymbol{k}_\perp - \boldsymbol{q})\,.$$

This integral equation translating $\hat{w}(q)$ into $\hat{C}^{\rm obs}_{\rm RM}(\boldsymbol{k}_\perp)$ has to be inverted in order to extract the former from the latter. Bayes' theorem states that the probability for a model (here the power-spectrum $\hat{w}(q)$) can be derived from the probability for the data (here the RM-map) given the model:

$P(\mathrm{model}|\mathrm{data}) \propto P(\mathrm{data}|\mathrm{model})\, P(\mathrm{model})$.

Maximizing this probability with respect to the model parameters provides the Maximum Likelihood power spectrum estimator. This technique

- is successfully used in CMB science and was tested for the Faraday application with mock RM data,
- requires Gaussianity of RM fluctuations, but this is expected due to the central limit theorem and is indeed indicated by observations,
- takes care of the influence of the window function, and
- provides errors and an error covariance matrix.

It also provides a general conceptual blueprint for extracting statistics of physically meaningful quantities from the statistics of the observed signal.

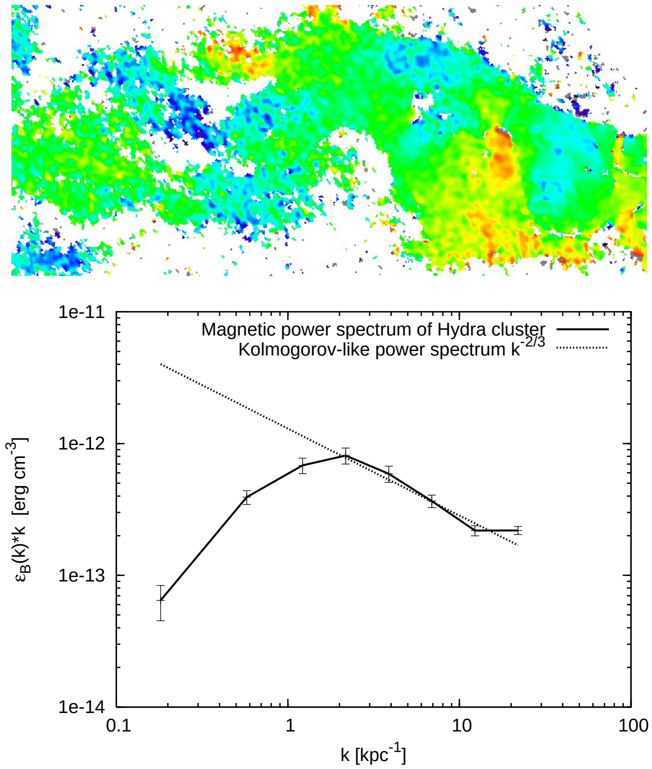

Fig. 2. Top: Faraday rotation map of the northern lobe of Hydra A (data: Taylor et al. (1990), map: Vogt et al. (2005)). Bottom: Faraday-based magnetic power spectrum of Hydra A cool core (Vogt & Enßlin (2005)).

4.2. Stokes correlators and Lorentz forces

Planck will provide high-accuracy and Faraday-free polarization maps. Are physically meaningful quantities encoded in them?

Eilek (1989) proposed to use correlation functions of Stokes parameters (henceforth Stokes correlators) to measure magnetic power spectra. Since the power spectra are two-point *second-order* statistics, while the Stokes correlators are two-point *fourth-order* statistics, the latter cannot be translated into power spectra without some closure assumptions. Eilek (1989) demonstrated how this works for a Gaussian closure. However, MHD turbulence is not likely to be well represented by Gaussian fluctuations. This is evident from the appearance of coherent structures like flux sheets and filaments in numerical simulations (Fig. 3) and from the observation of filamentary magnetic fields in galaxy clusters (Clarke & Enßlin, these proceedings).

If we were to look for physically meaningful quantities that are directly contained in the polarized emission data, the most obvious candidate is the Lorentz force

$$\frac{1}{c}\,\boldsymbol{J}\times\boldsymbol{B} = -\nabla\frac{B^2}{8\pi} + \frac{1}{4\pi}\,\boldsymbol{B}\cdot\nabla\boldsymbol{B}.$$

Since the Lorentz force is a quadratic quantity, its correlation function is a two-point fourth-order statistic. In the above expression, the first term on the right-hand side is the magnetic pressure force, the second term is the magnetic tension force

$$\boldsymbol{F} = \frac{1}{4\pi}\,\boldsymbol{B}\cdot\nabla\boldsymbol{B},$$

which not only determines the dynamical response of curved magnetic fields on the plasma, but can also be used to diagnose the structure of the field: the tension-force correlator measures the gradients of the field along itself. Thus, $\langle\boldsymbol{F}(\boldsymbol{x})\cdot\boldsymbol{F}(\boldsymbol{x}+\boldsymbol{r})\rangle$ can be used as one of the quantitative measures of the folded structure evident in Fig. 3, where the field varies across itself on a much larger scale than along itself. Further discussion, as well as numerical measurements of the tension-force statistics can be found in Schekochihin et al. (2004) (see also the review by Schekochihin & Cowley (2005)). We propose to study the statistics of the tension force using polarized radio observations.

The correlation tensor of the tension-force or its Fourier counterpart

$$\frac{1}{V}\langle\hat{F}_i(\boldsymbol{k})\overline{\hat{F}_m(\boldsymbol{k})}\rangle \;=\; k_j k_n \hat{C}_{ij,mn}(\boldsymbol{k})$$

where $\hat{C}_{ij,mn}(\boldsymbol{k})$ is the Fourier-space representation of the two-point fourth-order magnetic correlation tensor

$$C_{ij,mn}(\boldsymbol{r}) = \langle B_i(\boldsymbol{x})B_j(\boldsymbol{x})B_m(\boldsymbol{x}+\boldsymbol{r})B_n(\boldsymbol{x}+\boldsymbol{r})\rangle.$$

A general isotropic fourth-rank tensor depends on 26 scalar functions $C_{1\ldots26}(r)$ of the distance $r=|\boldsymbol{r}|$. Fortunately, tensor symmetries allow this set to be reduced to seven unknown scalar functions that fully determine the two-point fourth-order statistics of the field. In Fourier space, this reads

$$\hat{C}_{ij,mn}(k) = \hat{C}_1(k)\delta_{ij}\delta_{mn} + \hat{C}_2(k)(\delta_{im}\delta_{jn}+\delta_{in}\delta_{jm})$$
$$+\,\hat{C}_3(k)\hat{k}_i\hat{k}_j\hat{k}_m\hat{k}_n + \hat{C}_4(k)(\delta_{ij}\hat{k}_m\hat{k}_n+\delta_{mn}\hat{k}_i\hat{k}_j)$$

$$+ \hat{C}_5(k)(\delta_{im}\hat{k}_j\hat{k}_n + \delta_{in}\hat{k}_j\hat{k}_m + \delta_{jm}\hat{k}_i\hat{k}_n + \delta_{jn}\hat{k}_i\hat{k}_m)$$
$$+ i\hat{C}_6(k)(\epsilon_{imp}\hat{k}_p\delta_{jn} + \epsilon_{inp}\hat{k}_p\delta_{jm} + \epsilon_{jmp}\hat{k}_p\delta_{in} + \epsilon_{jnp}\hat{k}_p\delta_{im})$$
$$+ i\hat{C}_7(k)(\epsilon_{imp}\hat{k}_p\hat{k}_j\hat{k}_n + \epsilon_{inp}\hat{k}_p\hat{k}_j\hat{k}_m + \epsilon_{jmp}\hat{k}_p\hat{k}_i\hat{k}_n + \epsilon_{jnp}\hat{k}_p\hat{k}_i\hat{k}_m),$$

where $\hat{C}_{1\ldots7}(k)$ are all real. Is it possible to reconstruct these seven functions from observations? The accessible observables are the Stokes parameters. These are related to the magnetic fields in the emission region for Faraday-free, steep spectrum ($\alpha \approx -1$) radio emission:[1]

$$I(\boldsymbol{x}_\perp) = \int_{z_0}^{\infty} dz \left[B_x^2(\boldsymbol{x}) + B_y^2(\boldsymbol{x})\right]$$
$$Q(\boldsymbol{x}_\perp) = \int_{z_0}^{\infty} dz \left[B_x^2(\boldsymbol{x}) - B_y^2(\boldsymbol{x})\right]$$
$$U(\boldsymbol{x}_\perp) = \int_{z_0}^{\infty} dz\, 2\, B_x(\boldsymbol{x}) B_y(\boldsymbol{x}),$$

from which we can construct six scalar Stokes correlators: in Fourier space, $\hat{\Sigma}_{II}(\boldsymbol{k}_\perp)$, $\hat{\Sigma}_{QQ}(\boldsymbol{k}_\perp)$, $\hat{\Sigma}_{UU}(\boldsymbol{k}_\perp)$, $\hat{\Sigma}_{IQ}(\boldsymbol{k}_\perp)$, $\hat{\Sigma}_{IU}(\boldsymbol{k}_\perp)$, and $\hat{\Sigma}_{QU}(\boldsymbol{k}_\perp)$. These can be expressed as linear combinations of the scalar functions $\hat{C}_{1\ldots5}$, while $\hat{C}_6$ and $\hat{C}_7$ remain indeterminable. It turns out that the Stokes correlators are not independent and only four scalar correlation functions are, in fact, available from observations. Thus, we are short by one such function to fully reconstruct $\hat{C}_{1\ldots5}$.

Despite this scarcity of observable information, the power spectrum of the tension force happens to be fully observable! It is completely expressed in terms of the Stokes correlators:

$$\frac{1}{V}\langle \hat{\boldsymbol{F}}(\boldsymbol{k}_\perp)\cdot\overline{\hat{\boldsymbol{F}}(\boldsymbol{k}_\perp)}\rangle = \frac{\boldsymbol{k}_\perp^2}{8\pi}\int_0^{2\pi} d\varphi \Big[\hat{\Sigma}_{II}(\boldsymbol{k}_\perp) + 3\hat{\Sigma}_{QQ}(\boldsymbol{k}_\perp) - \left(\hat{\Sigma}_{QQ}(\boldsymbol{k}_\perp) - \hat{\Sigma}_{UU}(\boldsymbol{k}_\perp)\right)\cos 4\varphi + 4\hat{\Sigma}_{IQ}(\boldsymbol{k}_\perp)\cos 2\varphi\Big],$$

where φ is the angle between $\boldsymbol{k}_\perp$ and the x axis. This demonstrates that physically relevant information on MHD turbulence is encoded in the Stokes correlators and, therefore, can be obtained from Planck polarization data! The feasibility of this approach and the reliability of the underlying assumptions clearly require further careful investigation, which is currently underway.

5. Conclusions

1. The Planck surveyor mission is a high-precision experiment to study cosmology with the CMB.
2. However, an unambiguous detection with Planck of primordial magnetic fields — both from their imprint in the CMB power spectra and from their Faraday rotation — will be extremely challenging. But interesting constraints should be possible.
3. Galactic magnetic fields can well be studied by Planck via synchrotron, Faraday, and dust polarimetry, allowing a model-based reconstruction of large-scale fields.
4. Studying magnetic turbulence with Planck is promising: a new technique of Stokes correlators may allow us to measure the Lorentz-force power spectra in MHD turbulence, similar to the Faraday-based magnetic power spectra estimates.

[1] Here constant factors converting field strength to radio emissivity have been suppressed for simplicity of the calculations.

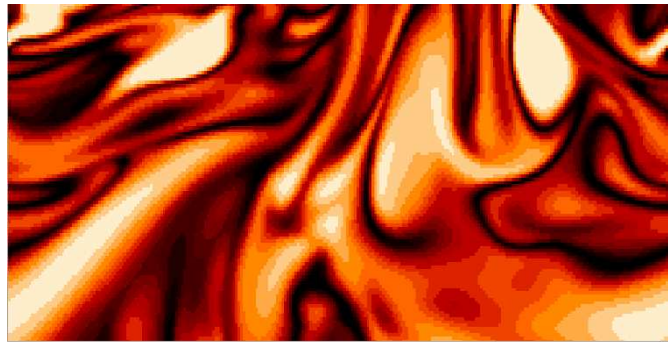

Fig. 3. Cross section of the field strength in the saturated state of a simulation of homogeneous isotropic MHD turbulence (run B in Schekochihin et al. (2004)).

Acknowledgements. TAE thanks the SOC for the invitation to and the LOC for the warm hospitality at this exciting conference. This work has benefited from research funding from the European Community's sixth Framework Programme under RadioNet R113CT 2003 5058187. AAS was supported by the UKAFF Fellowship.

References

Cordes, J. M., & Lazio, T. J. W. 2002, ArXiv Astrophysics e-prints, arXiv:astro-ph/0207156
Draine, B. T., & Lazarian, A. 1998, ApJ 494, L19
Eilek, J. A.: 1989, AJ98, 256
Enßlin, T. A., & Vogt, C.: 2003, A&A 401, 835
Fosalba, P. , Lazarian, A. , Prunet, S., Tauber, J.: 2001, in: S. Cecchini et al. (eds.), *Proc. of AIP Conf. Astrophysical Polarized Backgrounds*
Giovannini, M. 2005, ArXiv Astrophysics e-prints, arXiv:astro-ph/0508544
Górski, K. M., Hivon, E., Banday, A. J., Wandelt, B. D., Hansen, F. K., Reinecke, M., & Bartelmann, M. 2005, ApJ 622, 759
Jedamzik, K., Katalinić, V., & Olinto, A. V. 1998, PRD 57, 3264
Kosowsky, A., Kahniashvili, T., Lavrelashvili, G., & Ratra, B. 2005, PRD 71, 043006
Schekochihin, A.A., Cowley, S.C., Taylor, S.F., Maron, J.L., MacWilliams, J.C.: 2004, ApJ 612, 276
Schekochihin, A.A., Cowley, S.C.: 2005, in: S. Molokov, R. Moreau, H.-K. Moffatt (eds.), *Magnetohydrodynamics: Historical Evolution and Trends,* Springer, Berlin, in press (astro-ph/0507686)
Subramanian, K., & Barrow, J. D. 1998, PhRvL 81, 3575
Taylor, G. B., Perley, R. A., Inoue, M., Kato, T., Tabara, H., & Aizu, K. 1990, ApJ 360, 41
The Planck Bluebook, "The Scientific Program of Planck", The Planck Consortia: 2005, in press at the ESA Publication Division
Vogt, C., & Enßlin, T. A.: 2005, A&A 434, 67
Vogt, C., Dolag, K., & Enßlin, T. A. 2005, MNRAS 358, 732
Waelkens, A. 2005, Diploma thesis, Ludwig-Maximilian-Universität München